East European Journal of Physics. 4. 267-273 (2023)
DOI:10.26565/2312-4334-2023-4-33 ISSN 2312-4334

MICROSTRUCTURE, NANO-, AND MACRO-INDENTATION CHARACTERIZATION OF AISI 302 STEEL AFTER HIGH-TEMPERATURES AGING

Omar Ben Lenda[a,*], Hajar El Ganich[b], El Madani Saad[a]
[a] *Laboratory of Physical-Chemistry of Processes and Materials, Faculty of Sciences and Technology Settat, Hassan 1st University, Settat, Morocco*
[b] *Hassan First University of Settat, High Institute of Health Sciences, Laboratory of Sciences and Health Technologies, BP 555, 26000, Settat, Morocco*
**Corresponding Author e-mail: o.benlenda@uhp.ac.ma*
Received August 2, 2023; revised September 18, 2023; accepted September 19, 2023

The structural and mechanical studies of the AISI 302 steel aim to design a correct heat treatment in order to optimize its mechanical properties. In this study, we investigated the influence of temperature and time of aging on the structural and mechanical characteristics of the AISI 302 steel. The steel was aged at temperatures of 1100°C and 1200°C and for times ranging from 0 to 6000 minutes. The structural and mechanical characterization techniques used were the metallurgical microscope, nanoindentation technique, and macro-hardness test. At the microstructural level, an increase in the time or temperature of the aging contributed to an increase in the austenite grains size of AISI 302 steel. This microstructural change led to a decrease in the nanohardness and a drop in the macro-hardness between the unaged and aged conditions of AISI 302 steel.
Keywords: *AISI 302 Steel; Aging; Microstructure; Austenite; Grain growth; Nanohardness; Nanoindentation; Macro-hardness*
PACS: 81.05.Bx; 81.40.Cd; 81.70.Bt; 81.70.Fy

1. INTRODUCTION

In terms of annual production, austenitic stainless steels are the largest group of stainless steels [1]. The AISI 300 steel series are Chromium-Nickel alloys [2], which are essentially developed from steel composed of 18 wt% (percentage by weight) of Chromium and 8 wt% of Nickel [3]. They exhibit good mechanical properties, manufacturability, and corrosion resistance [1]. They are typically used in high-temperatures and food contact applications [4].

Owing to their importance at the industrial level, steels have been extensively studied to understand their metallurgical behavior [5-10]. In the literature, the phenomenon of austenite grain growth and its relationship with the temperature and time of the aging treatment have gained great interest [11–13]. D. Dong et al. [11], Z. Li et al. [12] and S. Benmaziane et al. [13] found that the austenite grain size of the steels increases considerably by increasing the treatment temperature. For a fixed temperature, they also reported that the grain growth rate decreases with increasing treatment time. The mechanism of grain growth has been elucidated in several studies [12, 14–16]. As shown in the work of R.C. Chen et al. [15], the growth of austenite grain in 300 M steel results from the grain boundaries migrating by incrementing temperature from 900°C to 1150°C and time from 5 to 120 minutes. For the GCr15 bearing steel cast billet treated at a temperature range of 1000–1250°C and a holding time interval of 30–180 minutes, Z. Li et al. [12] explained that grain boundaries migrating process decrease the driving force for grain growth.

Studies have sought to determine the effect of the size of austenite grains on the nano- and macro-mechanical properties of steels [17–20]. S. Li et al. [18], G. Liu et al. [19], and our previous work [20] reported the thermal aging behavior of the micro-constituents of various stainless-steel grades. For the austenite, at temperatures below 800°C and for prolonged holding times, the measurements showed that nanohardness after aging was slightly influenced [18–20]. The paper results of Y. Su et al. [17] have shown that the increase of the austenite grains size contributed to the decrease in the strength and ductility of Novel 20LH5 austenitic stainless steel.

Several metallurgical studies have been conducted on AISI 302 steel; however, only limited research has been performed on the evolution of the nanohardness of austenite as a function of time at high-temperatures. The structural and mechanical studies of the AISI 302 steel help to determine a heat treatment correctly to optimize its mechanical performance. In this paper, the aging mechanism and microstructural variations of AISI 302 steel at temperatures 1100°C and 1200°C up to 6000 minutes were investigated. Herein, the microstructure of AISI 302 steel under different heat treatment conditions was visualized using metallurgical microscope. Mechanical characterization of the AISI 302 steel before and after aging was carried out using the nanoindentation technique and macro-hardness tests.

2. MATERIALS AND METHODS

2.1. Chemical Composition

The chemical composition (in wt%) of the as-received AISI 302 steel is shown in Table 1 [21]. The AISI 302 steel was obtained from a steel plant located in the city of Casablanca, Morocco. At the industrial level, the AISI 302

Cite as: O. Ben Lenda, H. El Ganich, E. Saad, East Eur. J. Phys. 4, 267 (2023), https://doi.org/10.26565/2312-4334-2023-4-33

commercial steel was produced in an electric arc furnace and hot-rolled to 10 mm thick plates. The AISI 302 steel samples used in the present study were rectangular in shape and had dimension of 25×25×10 mm^3.

Table 1. Chemical composition of AISI 302 steel

Element	Fe	Cr	C	Ni	Si	Mn	P
Percentage by weight (wt%)	72.81	18	0.15	8	0.4	0.61	0.03

2.2. Aging Treatments

The AISI 302 steel samples were aged using a SELECTA air furnace at a heating rate of 20°C per minute and temperature control with an accuracy of ± 1°C. First, the steel was aged at two temperatures 1100°C and 1200°C and for the following durations: 0 (unaged condition of the AISI 302 steel), 60, 600, 1000, and 6000 minutes. Then, the quenching of the samples was carried out in water up to a temperature of ~ 25°C (room temperature).

2.3. Metallurgical Observations

Prior to the metallurgical observations, the samples of AISI 302 steel were mechanically polished using abrasive papers with grain sizes of 320, 600, 1200, and 4000. The polishing was completed using diamond pastes with particle sizes of 1, 3, and 6 µm and suspended in distilled water. This mechanical preparation made it possible to remove the oxide layers formed during heat treatments and to obtain a mirror-polished surface.

The structure of AISI 302 stainless steel was visualized by chemical etching with dilute aqua regia solution (mixture of 5 mL HNO_3, 15 mL HCl, and 100 mL H_2O) and the rinsing was performed with bi-distilled water [22]. The structure of the AISI 302 steel was examined using an OPTIKA brand metallurgical microscope coupled with a high-resolution AIPTEK camera. The average grain size was measured by using the linear intercept method.

2.4. Nanoindentation Technique

Nanoindentation tests were performed using a Nanoindenter XP (CSM Instruments) tester with a Berkovich indenter of B-O 45 series (pyramidal diamond tip with a nominal angle of 65.3° between the vertical axis and each face) [23]. Nanoindentations were performed under a maximum load of 50000 µN and a dwell time of 5 seconds.

Analysis of the loading-unloading curves of the samples was performed using the method of Oliver and Pharr [24, 25]. Figure 1 shows a typical loading–unloading curve with an indication of the parameters used in this method. The h_c is the contact depth and can be calculated as follows:

$$h_c = h_{max} - \varepsilon \times \left(\frac{P_{max}}{S}\right). \quad (1)$$

Where P_{max} is the peak load, h_{max} is the indenter maximum penetration on the sample flat surface, ε is a constant (equal to 0.75 for Berkovich indenter), and S is the unloading curve tangent slope.

A_c is the contact projection area and can be expressed as follows:

$$A_c = 24.5 \times {h_c}^2 + \sum_{i=0}^{7} C_i \times {h_c}^{1/2^i}. \quad (2)$$

Where C_1, C_2, ..., C_7 are constants. The first term of equation (2) describes the perfect shape of the Berkovich indenter, and the second term describes deviations from Berkovich geometry due to the blunting tip.

H_{IT} is the nanohardness and expressed as follows:

$$H_{IT} = P_{max}/A_c. \quad (3)$$

Another parameter used in the evaluation of loading-unloading curves is h_r which refers to the indenter residual penetration. The value of the h_r parameter is the intersection of the unloading curve with the horizontal axis (see Figure 1).

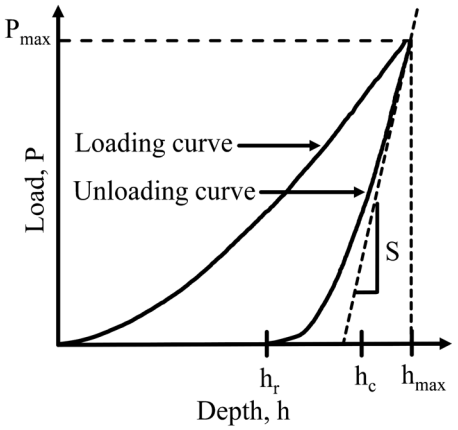

Figure 1. The typical loading-unloading curve of nanoindentation test

2.5. Macro-Hardness Test

Macro-hardness measurements were effectuated using a TESTWELL Durometer. The macro-hardness of the AISI 302 steel samples was evaluated using the ROCKWELL C method (diamond indenter with a total load of 150 Kgf) [26]. To assure repeatability, each macro-hardness value corresponded to the average of 10 indentations well distributed on the flat surface of each sample.

3. RESULTS AND DISCUSSIONS

3.1. Metallurgical Study

Figure 2 shows the phase fraction versus temperature diagram computed using the JMatPRO (version 7.0) software for the steel composition shown in Table 1 and for a temperature range of 1000 – 1500°C. As illustrated in Figure 2, the microstructure of AISI 302 steel was composed of 100 wt% of austenite for the two temperatures studied 1100°C and 1200°C.

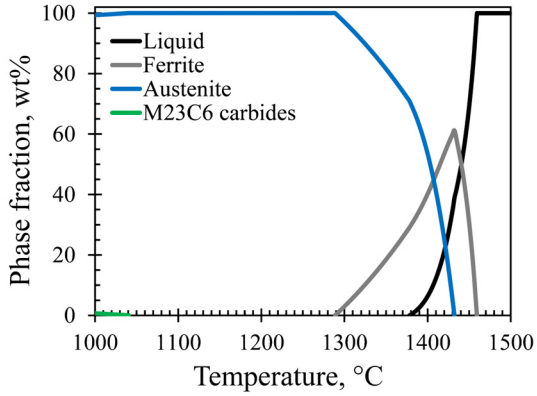

Figure 2. Phase diagram of the AISI 302 steel calculated using JMatPro (Version 7) software

Figure 3 shows micrographs of the microstructure of the AISI 302 steel aged at 1100 °C for 0, 60, 600, 1000, and 6000 minutes. According to the images obtained, the equiaxed grains size of the AISI 302 steel increased by increasing the aging time from 0 to 6000 minutes. The grains growth contributes to a reduction in the number of grains per unit volume, and therefore a decrease in the total area of grain boundaries [27]. At high-temperatures, these microstructural changes are caused by the grain boundaries migrating process [15–16].

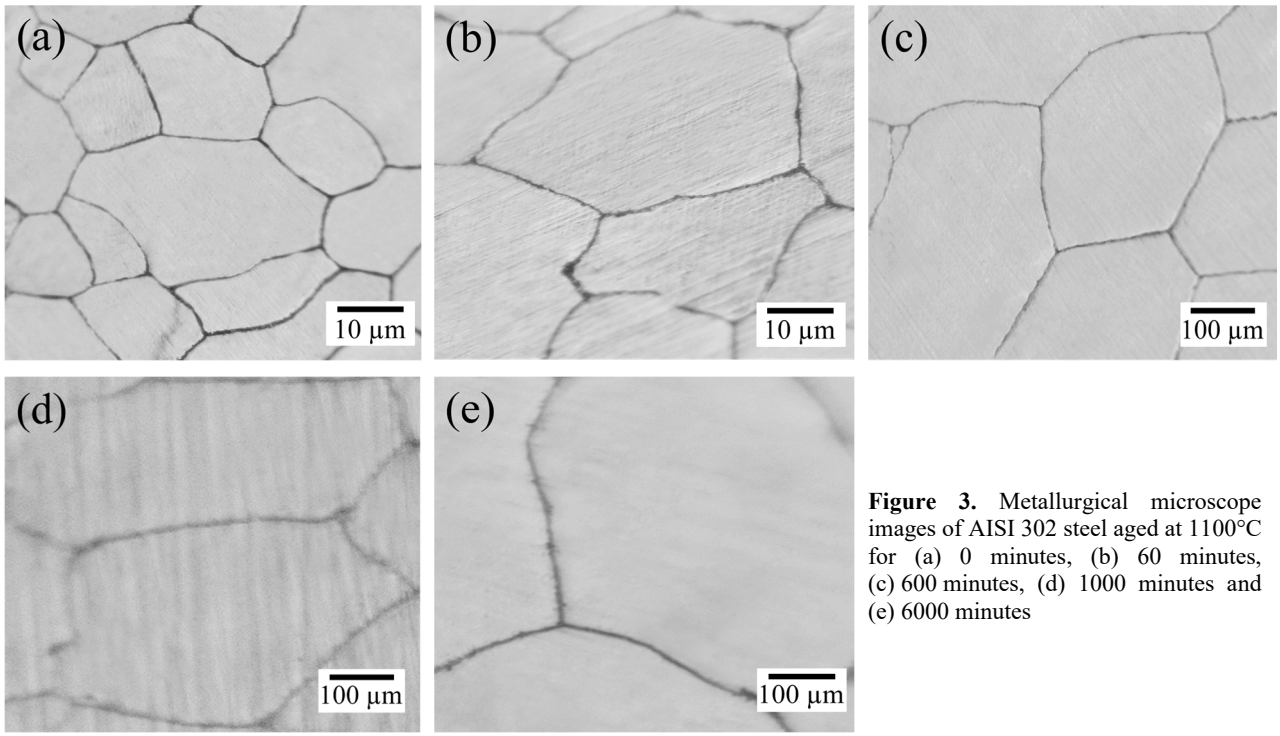

Figure 3. Metallurgical microscope images of AISI 302 steel aged at 1100°C for (a) 0 minutes, (b) 60 minutes, (c) 600 minutes, (d) 1000 minutes and (e) 6000 minutes

Figure 4 shows the austenite grain size as a function of the temperature and time of aging. As can be observed, for a fixed temperature, the austenite grain growth behavior can be divided into two stages: rapid growth stage for times below 1000 minutes, and relatively slow growth stage for times up to 6000 minutes. In other words, the majority of grain

growth occurred within 1000 minutes, and as the aging time increased, the grain growth rate slowed down. We can conclude that grain growth kinetics are reduced by increasing the aging time, which is linked to a decrease in the driving force for grain growth [28].

Several scientific papers have discussed the effect of the temperature and time of treatment on the austenite grain growth rate. The grain growth rate (dD/dt) can be quantitatively described as follows [12, 28-31]:

$$\frac{dD}{dt} = M_0 \exp\left(-\frac{Q_b}{R\,T}\right)\frac{A\,\gamma}{D}. \quad (4)$$

Where M_0 is the pre-exponential coefficient, Q_b is the grain boundary activation energy, R is the gas constant (8.314 J/mol/K), T is the temperature, A is a constant, γ is the grain boundary energy, and D is the austenite grain size. According to equation 4, the austenite growth rate increases with the increase of temperature and decreases with the increase of austenite grain size. These conclusions are in good agreement with the grain size measurements of AISI 302 steel under different conditions (see Figure 4).

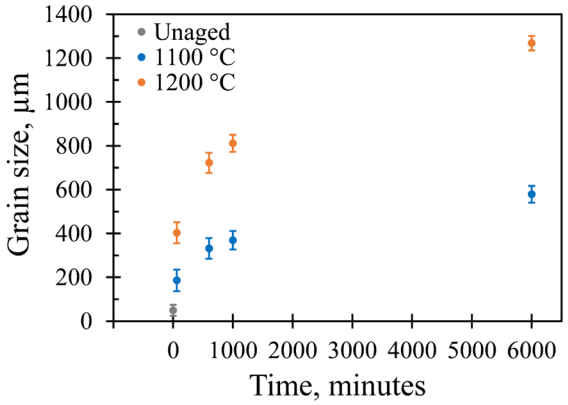

Figure 4. The austenite grain size of austenite aged at 1100°C and 1200°C for 0 (unaged), 60, 600, 1000, and 6000 minutes

3.2. Nanoindentation Technique

Figure 5 shows the nanoindentation curves of the austenite aged at 1100 °C and 1200°C for 0, 60, 600, 1000, and 6000 minutes. The nanoindentation measurements were categorized according to the aging temperature; Figure 5(a) for 1100°C and Figure 5(b) for 1200°C. The applied load (P) was plotted as a function of the penetration depth of the indenter (h) on the flat surfaces of the samples. For the different aging treatments, the mechanical behavior of the austenite was nearly identical. Nanoindentation curves did not exhibit discontinuities during the complete loading-unloading cycle [32, 33]. For all nanoindentation curves obtained, the unloading part was linear with a low slope. The plotted nanoindentation curves correspond to ductile materials [34].

We plotted the nanoindentation curve of the austenite aged for 0 minutes in Figure 5(a) and Figure 5(b) in order to visualize the effect of thermal aging time. At a given temperature, the nanoindentation curves shifted to the right by incrementing the aging time. According to Figure 5, the difference in displacement between the austenite curves was small for times greater than 60 minutes at two temperatures 1100°C and 1200°C.

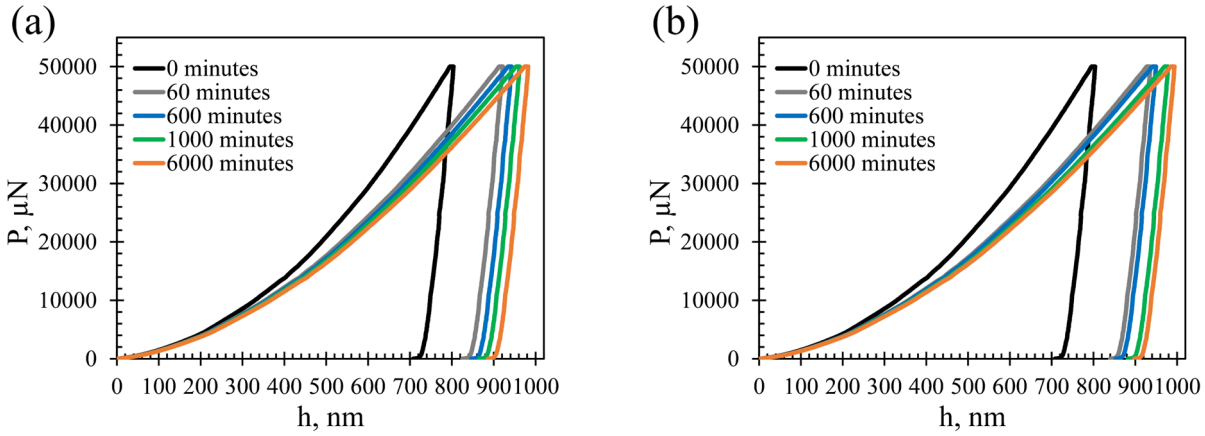

Figure 5. The loading-unloading curves of the AISI 302 steel
aged at (a) 1100°C and (b) 1200°C for 0 (unaged), 60, 600, 1000, and 6000 minutes

The nano-mechanical behavior of the austenite can also be evaluated from the parameters extracted from the P-h curves and which are h_{max} and h_r. Table 2 shows the values of the parameters h_{max} and h_r as a function of the

temperature and time of the aging. Compared to the austenite aged for 0 minutes, the values of h_{max} and h_r increased by increasing one of the aging treatment parameters (time or temperature).

Table 2. Parameters extracted from the loading-unloading curves of austenite aged at 1100°C and 1200°C for 0 (unaged), 60, 600, 1000, and 6000 minutes

	Maximum indenter penetration depth (h_{max} (nm))		Residual indenter penetration depth (h_r (nm))	
Aging time (minutes)	1100°C	1200°C	1100°C	1200°C
0 (unaged)	803.99		707.79	
60	921.71	936.15	825.51	839.95
600	942.81	949.62	846.61	853.42
1000	961.93	978.54	865.73	882.34
6000	982.36	994.10	886.16	897.90

Table 3 shows the variation in the elastic deformation work (W_e), plastic deformation work (W_p), and total work (W_t) performed by the Berkovich indenter in the austenite phase as a function of the temperature and time of the aging. The W_e corresponds to the area surrounded between the unloading curve and the horizontal axis. The W_p corresponds to the area between the loading and unloading curves and the horizontal axis. The W_t is the sum of the W_e and W_p. As can be seen from this table, the W_e decreased while the W_t and W_p increased by incrementing the temperature or time of the aging. These results indicated an increase in the plastic deformation of the austenite aged at temperatures 1100°C and 1200°C for the longest holding time of 6000 minutes.

Table 3. The elastic deformation work, plastic deformation work and total deformation work carried out by the Berkovich indenter at aging temperatures 1100°C and 1200°C for 0 (unaged), 60, 600, 1000, and 6000 minutes.

	Elastic work deformation carried out by the indenter (W_e (PJ))		Plastic work deformation carried out by the indenter (W_p (PJ))		Total work deformation carried out by the indenter (W_t (PJ))	
Aging time (minutes)	1100°C	1200°C	1100°C	1200°C	1100°C	1200°C
0 (unaged)	1869.49		12454.95		14324.44	
60	1723.60	1709.22	15401.94	16202.61	16725.54	17911.83
600	1704.09	1699.53	16465.45	16671.93	18169.54	18371.46
1000	1698.71	1678.84	16984.51	17256.79	18683.22	18935.63
6000	1661.42	1654.74	17322.82	17952.25	18984.24	19606.99

The nanohardness values of the austenite as a function of the temperature and time of the aging are summarized in Table 4. For a given aging time, the nanohardness at 1200°C was lower than that at 1100°C. For the two temperatures explored, the nanohardness of the austenite decreased for aging times between 0 and 60 minutes. By contrast, the nanohardness of the austenite remained nearly constant over an aging time interval ranging from 60 to 6000 minutes. Several scientific studies have also shown that the nano-hardness of the aged austenite is almost constant at temperatures between 350°C and 800°C, and for prolonged holding times up to 20000 h [35-37].

Table 4. Nano-hardness of the austenite aged at 1100°C and 1200°C for 0 (unaged), 60, 600, 1000, and 6000 minutes.

	Nanohardness (H_{IT} (GPa))	
Aging time (min)	1100°C	1200°C
0 (unaged)	3.69 ± 0.30	
60	2.75 ± 0.25	2.66 ± 0.30
600	2.62 ± 0.25	2.58 ± 0.25
1000	2.51 ± 0.15	2.42 ± 0.20
6000	2.40 ± 0.10	2.34 ± 0.15

3.3. Macro-Hardness Test

Figure 6 shows the macro-hardness evolution of the AISI 302 steel aged at 1100°C and 1200°C for 0, 60, 600, 1000, and 6000 minutes. Regardless of the aging temperature, this mechanical property reduced significantly by incrementing the treatment time.

As shown in Figure 6, the thermal aging behavior of AISI 302 steel was almost identical for the two temperatures studied. The aging behavior of the AISI 302 steel exhibited a decreasing trend with two-softening stages and it can be described as follows: the macro-hardness decreased sharply in the first stage (0–1000 minutes) and it continued to decrease but slightly in the second stage (1000–6000 minutes). The error bars represent the standard deviation of the macro-hardness measurements. In the second stage, the variation of the macro-hardness standard deviation fluctuated very little compared with the first stage.

The significant loss of the steel macro-hardness can be explained mainly by the austenite grains growth and reduction in the area of grain boundaries per unit volume [14,27,38]. The Hall-Petch equation [39–41] also confirms the relationship between the variation in the macro-hardness (H) and the change in the microstructure. It can be written as follows:

$$H = f \times \left(H_0 + {}^{k}\!/_{d^{\frac{1}{2}}} \right) + (1 - f) \times H_{GB}\,. \tag{5}$$

In which f is the volume fraction of the grains and (1-f) is the volume fraction of the grain boundaries, H_0 and k are material-specific constants, d is the average grain diameter, and H_{GB} is the hardness of the grain boundaries.

For the two temperatures investigated, the two stages of the macro-hardness variation as a function of time are due to the decrease of the grain growth rate by incrementing the treatment time [11, 12].

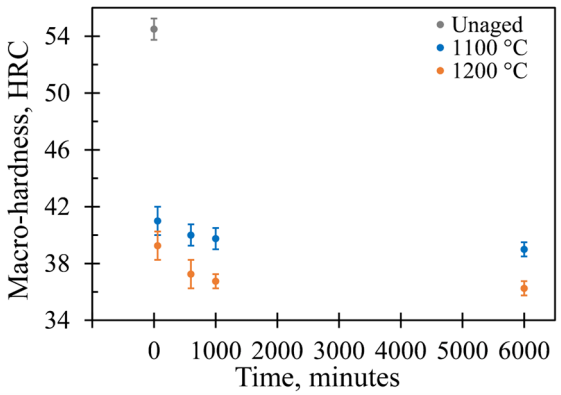

Figure 6. Macro-hardness variation of the AISI 302 steel aged at 1100°C and 1200°C for 0 (unaged), 60, 600, 1000, and 6000 minutes

4. CONCLUSIONS

In this study, the influence of thermal aging on the microstructural changes, nanoindentation responses, and macro-hardness evolution of the AISI 302 steel was investigated. The main conclusions drawn from this study were as follows:

1. According to metallurgical observations, the increase in the temperature or time of aging leads to an increase in the grains size. The austenite grain size aged for 0 minutes was 49.23 ± 25 µm and after 6000 minutes, it changed significantly to 581.71 ± 38.25 and 1268.10 ± 33.45 µm for the temperatures 1100°C and 1200°C, respectively.
2. At a fixed aging temperature, the nanohardness of the austenite decreased by incrementing the aging time from 0 to 6000 minutes. The nanohardness of the austenite aged at 0 minutes was equal to 3.69 ± 0.30 GPa, and after 6000 minutes of aging, it was equal to 2.40±0.10 and 2.34±0.15 GPa for the temperatures 1100°C and 1200°C, respectively.
3. For the temperatures explored, the macro-hardness property dropped significantly with incrementing the thermal aging time. The macro-hardness of AISI 302 steel aged at 0 minutes was equal to 54.5 ± 0.75 HRC and after 6000 minutes of aging, it was equal to 39 ± 0.5 and 36.25 ± 0.5 HRC for the temperatures 1100°C and 1200°C, respectively.

ORCID

Omar Ben Lenda, https://orcid.org/0009-0008-1979-5508; **Hajar El Ganich**, https://orcid.org/0000-0003-3303-607X
El Madani Saad, https://orcid.org/0000-0003-3621-1339

REFERENCES

[1] J.K.L. Lai, C.H. Shek, and K.H. Lo, *Stainless steels: An introduction and their recent developments*, (Bentham Science Publishers, Beijing, China, 2012), pp. 23. https://doi.org/10.1007/978-1-84628-669-8
[2] J.R. Davis, *Alloy digest sourcebook: stainless steels*, (ASM international, Materials Park, Ohio, USA, 2000), p. 7.
[3] S.L. Chawla, *Materials selection for corrosion control*, (ASM international, Materials Park, Ohio, USA, 1993), p. 117.
[4] F. Cardarelli, *Materials Handbook: A Concise Desktop Reference*, 2nd ed. (Springer Science & Business Media, London, UK, 2008), p. 102. https://doi.org/10.1007/978-1-84628-669-8
[5] N.A. Savinkov, O.M. Bulanchuk, and A.A. Bizyukov, East. Eur. J. Phys. **3**, 102 (2021). https://doi.org/10.26565/2312-4334-2021-3-16
[6] I. Kolodiy, O. Kalchenko, S. Karpov, V. Voyevodin, M. Tikhonovsky, O. Velikodnyi, G.Tolmachova, R. Vasilenko, and G. Tolstolutska, East. Eur. J. Phys. **2**, 105 (2021). https://doi.org/10.26565/2312-4334-2021-2-07
[7] V. Voyevodin, M. Tikhonovsky, G. Tolstolutska, H. Rostova, R. Vasilenko, O. Kalchenko, N. Andrievska, and O. Velikodnyi, East. Eur. J. Phys. **3**, 93 (2020), https://doi.org/10.26565/2312-4334-2020-3-12
[8] N. Filonenko, A. Babachenko, and G. Kononenko, East Eur. J. Phys. **2**, 46 (2019), https://doi.org/10.26565/2312-4334-2019-2-07
[9] V.A. Belous, Yu.A. Zadneprovskiy, N.S. Lomino, I.S. Domnich, and T.I. Bevs, East Eur. J. Phys. **4**, 98 (2018), https://doi.org/10.26565/2312-4334-2018-4-12
[10] O. Ben lenda, S. Benmaziane, A. Tara, and E. Saad, E3S Web Conf. **297**, (2021), https://doi.org/10.1051/e3sconf/202129701044
[11] D. Dong, F. Chen, and Z. Cui, J. Mater. Eng. Perform. **25**, 152 (2016), https://doi.org/10.1007/s11665-015-1810-9
[12] Z. Li, Z. Wen, F. Su, R. Zhang, and Z. Li, J. Mater. Res. **31**, 2105 (2016), https://doi.org/10.1557/jmr.2016.248
[13] S. Benmaziane, O. Ben Lenda, S. Saissi, L. Zerrouk, and E. Saad, Recent Pat. Mech. Eng. **15**, 486 (2022), http://dx.doi.org/10.2174/2212797615666220816123154
[14] Z. B. Liu, X. Tu, X. H. Wang, J. X. Liang, Z. Y. Yang, Y. Q. Sun, and C. J. Wang, J. Iron Steel Res. Int. **27**, 732 (2020), https://doi.org/10.1007/s42243-020-00429-6

[15] R.C. Chen, C. Hong, J.J. Li, Z.Z. Zheng, and P.C. Li, Procedia Eng. **207**, 663 (2017), https://doi.org/10.1016/j.proeng.2017.10.1038
[16] C. Yue, L. Zhang, S. Liao, and H. Gao, J. Mater. Eng. Perform. **19**, 112 (2010), https://doi.org/10.1007/s11665-009-9413-y
[17] Y. Su, R. Song, T. Wang, H. Cai, J. Wen, and K. Guo, Mater. Lett. **260**, 1 (2020), https://doi.org/10.1016/j.matlet.2019.126919
[18] S. Li, Y. Wang, S. Li, H. Zhang, F. Xue, and X. Wang, Mater. Des. **50**, 886 (2013), https://doi.org/10.1016/j.matdes.2013.02.061
[19] G. Liu, Y. Wang, S. Li, and X. Wang, J. Mater. Eng. Perform. **27**, 4714 (2018), https://doi.org/10.1007/s11665-018-3540-2
[20] O. Ben Lenda, E. Saad, A. Tara, and O. Jbara, Adv. Mater. Process. Technol. **8**, 3859 (2022), https://doi.org/10.1080/2374068X.2022.2036443
[21] H.S. Khatak, and B. Raj, *Corrosion of Austenitic Stainless Steels: Mechanism, Mitigation and Monitoring* (Woodhead Publishing, Cambridge, UK, 2002), p. 6
[22] G.F. Vander Voort, *Metallography, Principles and Practice* (ASM International, Materials Park, Ohio, USA, 1999), p. 649
[23] M. Yovanovich, in: *Proceedings of the 44th AIAA Aerospace Sciences Meeting and Exhibit* (American Institute of Aeronautics and Astronautics, Reno, Nevada, 2006), pp. 1-28.
[24] W.C. Oliver, and G.M. Pharr, J. Mater. Res. **7**, 1564 (1992). https://doi.org/10.1557/JMR.1992.1564
[25] G.M. Pharr, W.C. Oliver, and F.R. Brotzen, J. Mater. Res. **7**, 613 (1992). https://doi.org/10.1557/JMR.1992.0613
[26] E. Broitman, Tribol. Lett. **65**, 1 (2017), https://doi.org/10.1007/s11249-016-0805-5
[27] G.E. Dieter, H.A. Kuhn, and S.L. Semiatin, *Handbook of Workability and Process Design* (ASM international, Materials Park, Ohio, USA, 2003), pp. 250-251
[28] Y. Xu, J. Liu, Y. Zhao, and Y. Jiao, Philos. Mag. **101**, 77 (2021). https://doi.org/10.1080/14786435.2020.1821113
[29] M. Militzer, E.B. Hawbolt, and T.R. Meadowcroft, Metall. Mater. Trans. A, **27**, 3399 (1996). https://doi.org/10.1007/BF02595433
[30] S.H. Mohamadi Azghandi, V. Ghanooni Ahmadabadi, and A. Zabett, Philos. Mag. **94**, 2758 (2014). https://doi.org/10.1080/14786435.2014.932460
[31] B.R. Patterson, and Y. Liun, Metall. Trans. A. **23**, 2481 (1992). https://doi.org/10.1007/BF02658051
[32] T.H. Ahn, C.S. Oh, K. Lee, E.P. George, and H.N. Han, J. Mater. Res. **27**, 39 (2012), https://doi.org/10.1557/jmr.2011.208
[33] N.K. Mukhopadhyay, and P. Paufler, Int. Mater. Rev. **51**, 209 (2006), https://doi.org/10.1179/174328006X102475
[34] O. Ben Lenda, A. Tara, F. Lazar, O. Jbara, A. Hadjadj, and E. Saad, Strength Mater. **52**, 71 (2020). https://doi.org/10.1007/s11223-020-00151-4
[35] S.L. Li, Y.L. Wang, and X.T. Wang, Mater. High Temp. **32**, 524 (2015). https://doi.org/10.1179/1878641314Y.0000000040
[36] G. Liu, Y. Wang, S. Li, K. Du, and X. Wang, Mater. High Temp. **33**, 15 (2016). https://doi.org/10.1179/1878641315Y.0000000014
[37] S.L. Li, Y.L. Wang, H.L. Zhang, S.X. Li, K. Zheng, F. Xue, and X.T. Wang, J. Nucl. Mater. **433**, 41 (2013). https://doi.org/10.1016/j.jnucmat.2012.09.004
[38] J. Choi, C.S. Seok, S. Park, and G. Kim, J. Mater. Res. Technol. **8**, 2011 (2019). https://doi.org/10.1016/j.jmrt.2018.11.017
[39] E.O. Hall, Proc. Phys. Soc. B, **64**, 747 (1951). https://doi.org/10.1088/0370-1301/64/9/303
[40] N.J. Petch, J. Iron Steel Inst. **174**, 25 (1953)
[41] A.M. Glezer, and I.E. Permyakova, *Melt-Quenched Nanocrystals* (CRC Press, Boca Raton, Florida, USA, 2013).

ХАРАКТЕРИСТИКА МІКРОСТРУКТУРИ, НАНО- ТА МАКРОІНДЕНТАЦІЇ СТАЛІ AISI 302 ПІСЛЯ ВИСОКОТЕМПЕРАТУРНОГО СТАРІННЯ

Омар Бен Ленда[a], Хаджар Ель Ганіч[b], Ель Мадані Саад[a]

[a] *Перший університет Хасана в Сетаті, лабораторія фізико-хімії процесів та матеріалів факультету наук та технологій, Сетат, Марокко*

[b] *Перший університет Хасана в Сеттаті, вищий інститут медичних наук, лабораторія наук та технологій охорони здоров'я, BP 555, 26000, Сетат, Марокко*

Структурні та механічні дослідження сталі AISI 302 спрямовані на розробку правильної термообробки з метою оптимізації її механічних властивостей. У цьому дослідженні ми досліджували вплив температури та часу старіння на структурно-механічні характеристики сталі AISI 302. Сталь старіли при температурах 1100°C і 1200°C протягом часу від 0 до 6000 хвилин. Методами структурної та механічної характеристики, які використовувалися, були металургійний мікроскоп, метод наноіндентування та тест на макротвердість. На мікроструктурному рівні збільшення часу або температури старіння сприяло збільшенню розміру зерен аустеніту сталі AISI 302. Ця зміна мікроструктури призвела до зниження нанотвердості та падіння макротвердості між нестареним і старим станом сталі AISI 302.

Ключові слова: *сталь AISI 302; старіння; мікроструктура; аустеніт; зростання зерна; нанотвердість; наноіндентування; макротвердість*